Textures and Microstructures, 1991, Vols 14–18, pp. 909–914
Reprints available from the publisher
Photocopying permitted by license only

TEXTURES OF WARM ROLLED LOW CARBON AND TITANIUM BEARING EXTRA LOW CARBON STEEL SHEETS

T. SENUMA*, H. YADA*, R.SHIMIZU* and J.HARASE*
*R&D Laboratories III, Nippon Steel Corporation, Kitakyushu, Japan, 805

1.INTRODUCTION

In this work, the formation of textures of low carbon and Ti-bearing extra low carbon steel sheets warm rolled in the temperature range between 900K and 1050K have been investigated through microscopic and microtextural studies using the ECC-ECP (electron chanelling contrast - electron channeling pattern) techniques and selected area diffraction patterns to explain the different features of texture formation in the two steels and the effect of carbon in solution on the texture formation is discussed.

2.EXPERIMENTAL PROCEDURE

The chemical compositions of the Ti bearing extra low carbon steel (Steel A) and the low carbon steel (Steel B) used here are given in Table 1.

Table.1: Chemical compositions of steels used in the experiment.

Steel	C	Ti	Si	Mn	P	S	Al	N
A	0.0035	0.064	0.02	0.25	0.001	0.005	0.012	0.0023
B	0.0100	–	0.006	0.24	0.004	0.004	0.021	0.0020

The specimens were prepared as follows. Ingots of 50 kg melted in a laboratory vacuum furnace were heated and held at 1523K for 1 hour and hot rolled to 12mm thick plates at a finishing temperature of about 1273K. Test pieces 10mm thick, 50mm wide and 100mm long were machined from the plates. For the experiments, specimens were reheated and held at 1273K for 30 minutes and hot rolled 50% at about 1200K to refine the austenite grain structure. Subsequently, they were air cooled to a temperature of 1023K and then warm rolled at a reduction of 80% to 1mm thick sheet.

The recrystallization texture was measured from specimens annealed for 1 hour at 1023K while the warm rolling texture was determined from specimens quenched just after rolling.

The measurement of texture was carried out on an automatic goniometer with a Mo tube. Detailed studies of the texture have been performed by means of the three dimensional analysis based on the vector method/1,2/.

For the microtextural studies, the SEM-ECP technique was employed to determine the orientation of each grain observed at the initial stages of recrystallization.

Both ECP as well as selected area diffraction patterns were used to determine the changes in crystal orientation taking place in the deformed grains, especially in the vicinity of grain boundaries.

3. EXPERIMENTAL RESULTS

The onset temperature of recrystallization of Steel A at a constant heating rate of 10 °C/s.was about 80K higher than that of Steel B.

The carbon in Steel A was almost completely precipitated in the form of Ti compounds before the warm rolling. On the other hand, Steel B contained carbon in solution during warm rolling to approximately its total content of 100 ppm.

Fig.1 shows the rolling and recrystallization textures at the midplanes of Steels A and B warm rolled to 80% reduction at 1023K. Steel A developed a rather strong <111>//ND fiber in the rolling texture and these orientations became the main orientations of the recrystallization texture.

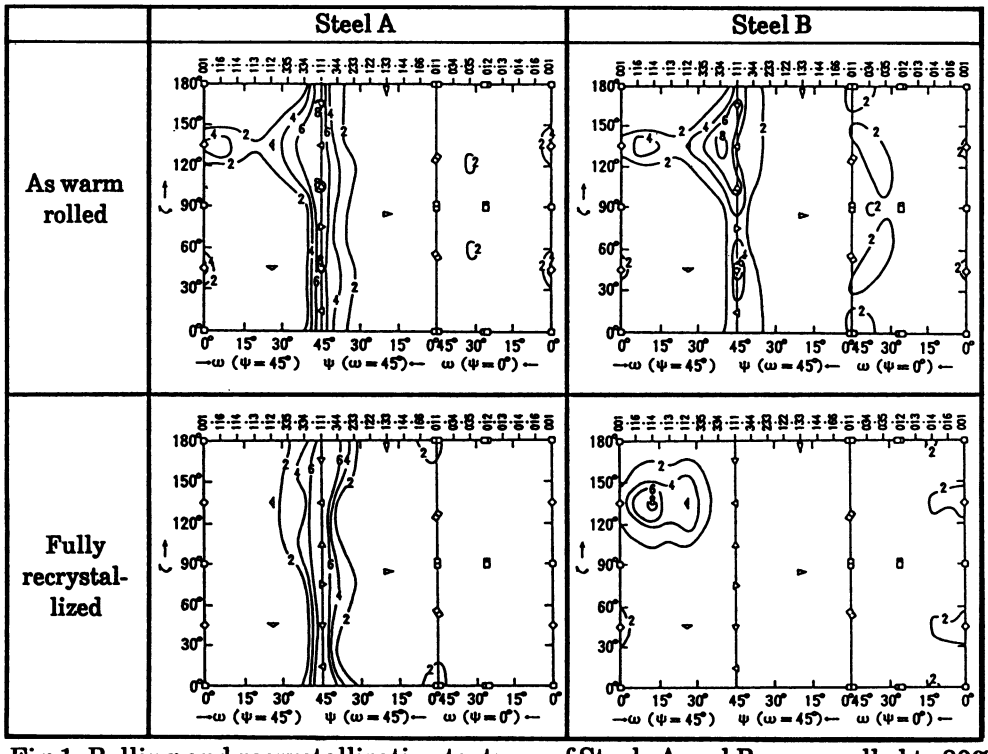

Fig.1: Rolling and recrystallization textures of Steels A and B warm rolled to 80% reduction at 1023K. Annealing was conducted at 1023K for 30 minutes.

On the other hand, the development of the <111>//ND fiber was in some measure hindered in the rolling texture of Steel B. The main orientation of the recrystallization texture was near {114}<110> and the <111>//ND fiber was negligibly weak.

To clarify the mechanism of formation of the different textures in the two steels, a detailed microstructural and microtextural study was carried out with specimens recrystallized about 5% using the ECC and ECP techniques.

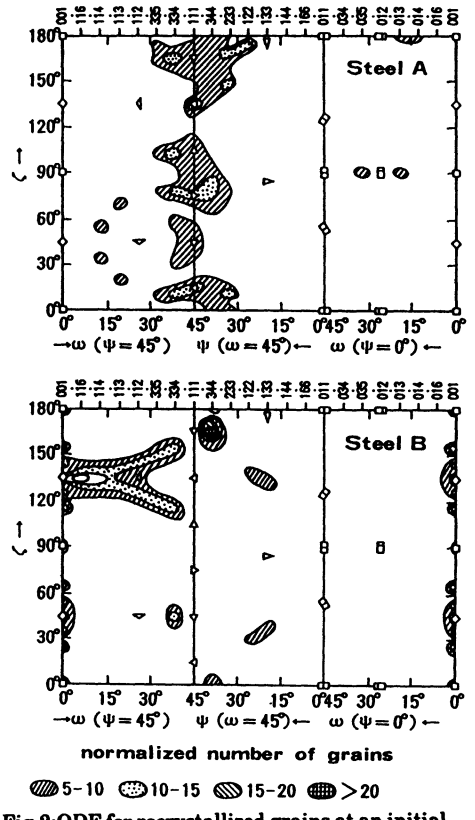

Fig.2:ODF for recrystallized grains at an initial stage of recrystallization. Orientations were determined by ECP. The numbers of grains involved were 221 and 336 for Steels A and B, respectively.

Table2: Classification of recrystallized grains.

Mark	Definition of recrystallized grains
XI	Nucleated within X grains
XX	Nucleated at grain boundaries between X grains
ZI	Nucleated within Z grains
ZZ	Nucleated at grain boundaries between Z grains
XZ-X	Recrystallized from X grains at the grain boundary between X and Z grains
XZ-Z	Recrystallized from Z grains at the grain boundary between X and Z grains
P	Nucleation site could not be identified.

Fig. 2 shows an orientation distribution diagram using ECP data of 221 and 336 grains observed in an arbitrary area of 0.6 x 1.0mm for Steels A and B, respectively. In this case, the intensity given in the diagram does not mean the fraction of area but that of number of the grains. It can be recognized that the recrystallization texture formed at the initial stage of recrystallization is approximately the same as that observed after complete recrystallization.

Microscopic observations by ECC show that the deformed grains can be roughly divided into two types. The grains of the first type, hereafter called X grains which have near <111>//ND orientations. The grains of the second type, hereafter called Z grains, are characterized by a recovered structure whose subgrain boundaries are vague. The orientations of the Z grains are near <100>//ND.

To investigate the relationship between the orientations of recrystallized grains and their nucleation sites, the latter were categorized as shown in Table 2.

Fig.3 illustrates the numbers of recrystallized grains identified at the various nucleation sites. In Steel A, recrystallized grains were nucleated mainly at the grain boundaries between X grains and within X grains, while

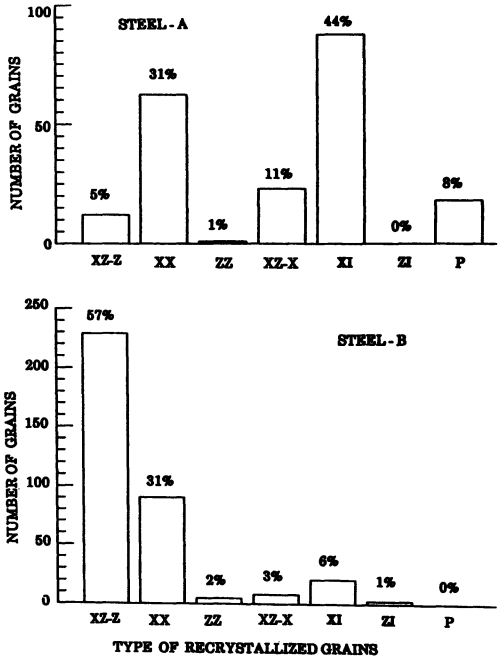

Fig.3: Number of recrystallized grains at different nucleation sites. The numbers of grains involved were 221 and 336 for Steels A and B, respectively.

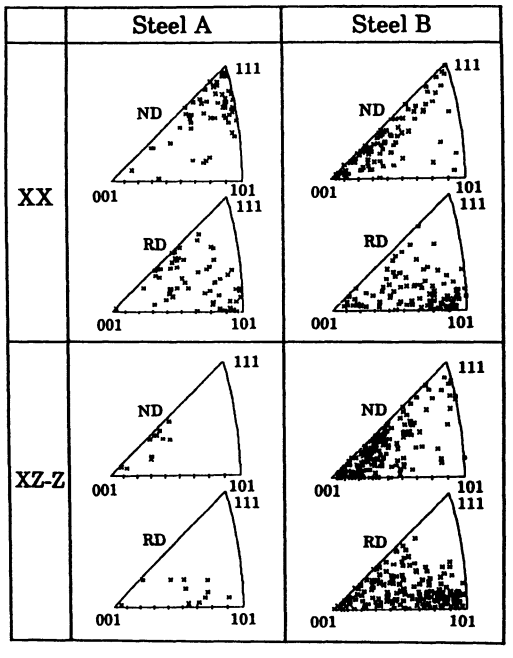

Fig.4: Orientations of the XX and XZ-Z grains in Steels A and B.
(ND: normal direction, RD: rolling direction)

nearly 60% of the nucleation sites in Steel B were at the grain boundaries between X and Z grains.

Fig.4 shows the orientations of the XX and XZ-Z grains. In Steel A, the orientations of the XX grains were mostly near <111>//ND, while in Steel B, the main orientations were near {115}-{112}<110>, although there were also some near<111>//ND. The main orientations of the XZ-Z grains were near {100}-{112}<110> for both steels, though the number of such grains in Steel A was much less than that in Steel B.

4. DISCUSSION

4.1 Influence of the retardation of recrystallization on the recrystallization texture

The difference in recrystallization behaviour between Steels A and B can be recognized from their preferred nucleation sites, as shown in Fig.3. One of the reasons why the near <100>//ND orientations did not develop in the recrystallization texture of Steel A is closely related to the fact that the recrystallization of XZ-Z grains was suppressed. Due to the small driving force, the recrystallization of XZ-Z grains can be easily suppressed if boundary migration is hindered by the solute drag effect or by the pinning effect caused by finely distributed precipitates. In the case of Steel A, the recrystallization of XZ-Z grains was suppressed by the above mentioned effects through the addition of Ti.

4.2. Effect of carbon in solution on the formation of texture

Selected area electron diffraction was employed to determine the orientation changes in the vicinity of the grain boundaries in the X grains. In Steel A, in which little carbon in solution was present, a rotation around <111>//ND was frequently observed in the vicinity of the grain boundaries between the X grains. This local rotation was also observed in a cold rolled low carbon steel sheet/3/ and the occurrence of this rotation was explained by the selection of active slip systems of the {110}<111> type, which is influenced by the stresses produced by slips in the neighbouring grains/4/.

On the other hand, other crystal rotations forming {112}<110>-{115}<110> orientations were frequently found in the vicinity of the grain boundaries between the X grains in Steel B but seldom in Steel A. Fig.5 shows such an example. The occurrence of this kind of crystal rotation is possibly explained by work hardening of the slip systems through the interaction of carbon in solution with dislocations as follows.

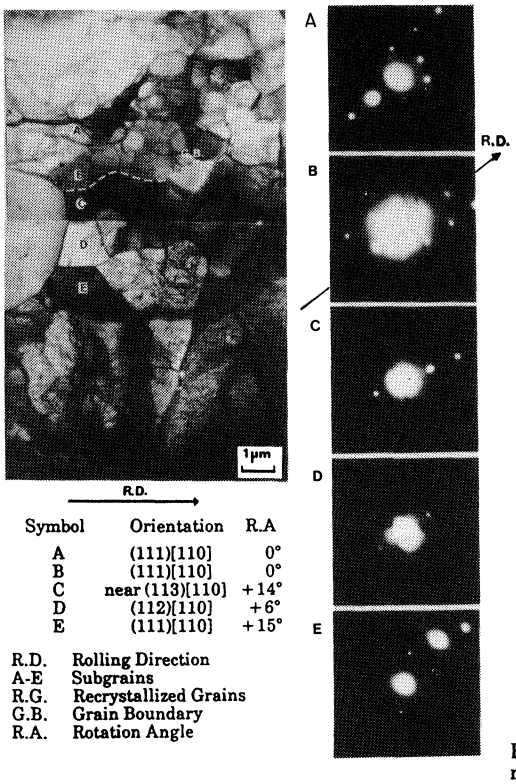

Symbol	Orientation	R.A
A	(111)[110]	0°
B	(111)[110]	0°
C	near (113)[110]	+14°
D	(112)[110]	+6°
E	(111)[110]	+15°

R.D. Rolling Direction
A-E Subgrains
R.G. Recrystallized Grains
G.B. Grain Boundary
R.A. Rotation Angle

Fig.5: Change in orientation in the vicinity of an grain boundary between X grains determined by selected area electron diffraction. Observations were made on a specimen of Steel B at a stage of about 5% recrystallization.

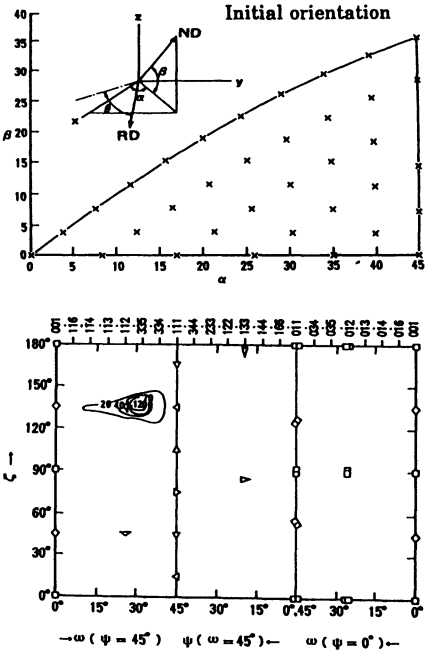

Fig.6: Crystal orientations calculated by crystal rotation models /5,6/ on the assumption that the first 60% rolling reduction occurs by pencil glide and the subsequent 50% deformation occurs solely by glide on the {112}<111> slip systems.

The probability of C-atoms lying in {110} planes is 1.73 times higher than that of lying in {112} planes, both of which are considered as the main slip planes in bcc crystals. It is therefore possible that dislocations pile up during deformation in the vicinity of grain boundaries and that the interaction

between dislocations and carbon in solution leads to more work hardening of the {110}<111> slip systems so that further deformation takes place mainly on the {112}<111> slip systems.

Fig.6 shows an orientation distribution diagram predicted by a crystal rotation model/5,6/ on the assumption that the first 60% rolling deformation occurs by means of pencil glide and the subsequent 50% only involves glide on the {112}<111> slip systems. The initial texture consists of 648 orientations representing the 36 planes given in the figure and 18 directions with an interval of 10°. As shown in the figure, the main orientations of the rolling texture are near {114}<110>-{335}<110>, which are orientations frequently observed in subgrains in the vicinity of the grain boundaries between the X grains in Steel B. The fact that the main orientations of the XX grains of Steel B coincided approximately with the orientations mentioned above strongly indicates that the recrystallization occurred from these subgrains.

5.Conclusion

The textures of warm rolled low carbon and Ti-bearing extra low carbon steel sheets have been investigated. The study led to the following conclusions:

1. The main orientations of grains recrystallized from deformed grains of near <111>//ND are near <111>//ND if carbon in solution is eliminated; they are {112}<110>-{115}<110> if carbon in solution is present.

2. The main orientations of grains recrystallized from deformed grains of near <100>//ND are {100}<110>-{112}<110>.

3. To suppress the recrystallization of deformed grains of near <100>//ND, the addition of recrystallization retarding elements such as Ti is effective.

4. The differences in the recrystallization textures formed in low carbon and Ti-bearing extra low carbon steel sheets can be explained by the differences in the local crystal rotations in the vicinity of grain boundaries and in the preferred nucleation sites.

5. To obtain recrystallization textures with near <111>//ND as the main orientation through warm rolling, which is good for the deep drawability, it is necessary to employ steels containing Ti, Nb etc. which retard recrystallization and eliminate carbon in solution by the formation of precipitates.

References

1) D. Ruer and R. Baro: J. Appl. Cryst., 10, 458 (1977)
2) R. Shimizu, K. Ohta and J. Harase: Textures and Microstructures, 10, 101 (1989)
3) H. Inagaki: Trans. Jap. Inst. Metals 28, 251 (1987)
4) H. Inagaki: Trans. ISIJ, 24, 266 (1984)
5) I. L. Dillamore and H. Katoh: Met. Sci., 8 (1974) 21
6)J. G. Sevillano, P. van Houtte and E. Aernoudt: Prog. Mater. Sci. 25, 69 (1981)